

Surface brightness profiles and structural parameters for globular clusters in the Fornax and Sagittarius dwarf spheroidal galaxies

A. D. Mackey^{1*} and G. F. Gilmore¹

¹*Institute of Astronomy, University of Cambridge, Madingley Road, Cambridge CB3 0HA*

Accepted – Received –

ABSTRACT

We present radial surface brightness profiles for all five globular clusters in the Fornax dwarf spheroidal galaxy, and for the four present members of the Sagittarius dwarf spheroidal galaxy. These profiles are derived from archival *Hubble Space Telescope* observations, and have been calculated using the same techniques with which we measured profiles in our previous studies of LMC and SMC clusters (Mackey & Gilmore 2002a,b), apart from some small modifications. From the surface brightness profiles, we have determined structural parameters for each cluster, including core radii and luminosity and mass estimates. We also provide a brief summary of literature measurements of other parameters for these clusters, including their ages, metallicities and distances.

Our core radius measurements are mostly in good agreement with those from previous lower resolution studies, although for several clusters our new values are significantly different. The profile for Fornax cluster 5 does not appear to be well fit by a King-type model and we suggest that it is a post core-collapse candidate. We examine the distribution of cluster core radii in each of the two dwarf galaxy systems, and compare these with the distribution of core radii for old LMC clusters. The three distributions match within the limits of measurement errors and the small sample sizes. We discuss the implications of this in the context of the radius-age trend we have previously highlighted for the Magellanic Cloud clusters.

Key words: galaxies: star clusters – globular clusters: general – galaxies: individual: Fornax dwarf spheroidal, Sagittarius dwarf spheroidal – Local Group – stars: statistics

1 INTRODUCTION

Recently, we (Mackey & Gilmore 2002a,b; hereafter Paper I and Paper II respectively) presented high resolution surface brightness profiles for a large sample of clusters in the Large and Small Magellanic Clouds (LMC and SMC respectively), as measured with the Wide Field Planetary Camera 2 (WFPC2) on the *Hubble Space Telescope* (*HST*). These two galaxies are locally unique in containing star clusters of comparable masses to the Milky Way’s globular clusters (see Papers I and II) but with ages ranging from the very newly formed ($\tau \sim 10^6$ yr) to those coeval with the oldest Galactic globulars ($\tau \geq 10^{10}$ yr). The LMC and SMC systems therefore permit direct observational studies of globular cluster evolution.

One aspect of this is reflected in the trend in cluster structure we highlighted in Papers I and II. When core radius (r_c) is plotted as a function of age, clusters in both systems follow a distinct distribution. The youngest clusters all have compact cores ($r_c \sim 1 - 2$ pc), with the upper envelope of r_c systematically increasing with age so that the oldest clusters exhibit a wide spread in their core sizes ($0 \leq r_c \leq 8$ pc). In Paper I, we showed that this trend is

almost certainly not the result of a selection effect or a correlation between other intrinsic properties of the clusters. Furthermore, de Grijs et al. (2002) showed that the radius-age distribution is not due to the comparison of profiles measured from different stellar masses – that is, the reduced spread in r_c for the youngest clusters cannot be a result of their profiles being dominated by a few high luminosity mass-segregated stars, because if only stars in the mass range $\sim 0.8 - 1.0M_\odot$ are used to repeat the measurements (for a subsample of the clusters) the radius-age distribution persists. It therefore seems that this observed distribution represents some genuine form of time dependent structural alteration in clusters in both Magellanic Clouds.

The means by which some clusters obtain significantly expanded cores while others do not remains unclear. In Paper I, we speculated on several physical processes which are known to alter the structure of stellar clusters, including the effects of mass loss due to stellar evolution and the regulatory influence of the initial mass function (IMF), the effects of heating due to three-body encounters and a significant population of binary stars, the possibility of extreme tidal effects from the parent galaxies, and the mergers of pairs of gravitationally bound clusters. However, for the reasons discussed in Paper I, none of these mechanisms seems to provide a viable means of reproducing the observed trend. Wilkinson et

* E-mail: dmackey@ast.cam.ac.uk

al. (2003) have attacked the problem from a computational point of view. Their N -body simulations have shown that it does indeed seem unlikely that significant populations of binary stars or extreme tidal influences can cause the necessary core expansion. This has led them to suggest that perhaps the observed trend reflects changing formation conditions rather than excessively dynamic cluster structures – an idea which we are presently following up via additional simulations.

A second avenue of exploration is to observe if the radius-age trend is present in any other globular cluster systems or whether it is unique to the atypical Magellanic systems, thereby shedding light on the possible evolutionary (or formation) conditions which might lead to the r_c distribution. There are only three other globular cluster systems which are near enough to allow study at sufficient resolution, and whose cluster censuses are (mostly) complete. These are the Milky Way globular clusters, and those of the Fornax and Sagittarius dwarf spheroidal (dSph) galaxies. The Galactic globular cluster system is extensive, with ~ 150 members, and shows evidence for a complicated history of both formation and accretion of clusters (see e.g., Zinn (1993)). A detailed study of this system is therefore beyond the scope of this paper, but will be presented in the future (Mackey & Gilmore, in prep.).

The Fornax and Sagittarius dSph galaxies are the two most massive of the ~ 11 dwarf galaxies associated with the Milky Way, and the only two to possess globular clusters (see e.g., Forbes et al. (2000)). Fornax contains five, while Sagittarius has four definite members, plus at least one (Pal 12, see e.g., Martínez-Delgado et al. (2002)) probably previously associated. Unlike the Magellanic globular clusters however, the Fornax and Sagittarius clusters are exclusively old ($\sim 7 \leq \tau \leq 15$ Gyr). It is therefore not possible to directly observe any radius-age trend for these two systems; however, we can measure the distribution of core radii and match it against that for the oldest Magellanic clusters – thereby observing whether clusters with expanded cores are present in the two systems, and in what proportion.

To this end, we have located WFPC2 observations of the Fornax and Sagittarius globular clusters in the *HST* archive, and put these data through the same reduction and surface brightness profile construction pipelines we established for the Magellanic Cloud clusters. This extends our group of directly comparable sets of measurements to all four of the closest globular cluster systems external to the Milky Way. We describe the data and list a set of parameters we have compiled from the literature for each cluster in Section 2, and briefly reiterate the reduction procedures in Section 3, as well as describing several alterations to this process which were required in order to deal with some of the characteristics of the new observations. In Section 4 we present our results, and discuss these in the context of the old Magellanic clusters in Section 5. The results from the present study (Tables 1, 2, 3, 4, 5, and 7) together with the surface brightness profiles, are available on-line at http://www.ast.cam.ac.uk/STELLARPOPS/dSph_clusters/.

2 THE CLUSTER SAMPLE

2.1 Observations

In order to ensure results from this reduction and analysis were directly comparable to the results from Papers I and II, we required observations in the same format as in these two studies – that is, in the general form of a cluster observed once (or in selected cases, multiple times) through the F555W filter, and once (or again, mul-

tle times) through a second filter. Two *HST* programs have observed Fornax dSph globular clusters with WFPC2 – program 5917 (Fornax 1, 2, 3, and 5) and program 5637 (Fornax 4). As described below in Section 3, because of the large distance of the Fornax system we required multiple exposures of each cluster, and hence we downloaded all the available data from these programs. The full data set is listed in Table 1. All clusters were observed through the F555W and F814W filters. For the clusters observed in program 5917, typical total exposure times were 5640 seconds in F555W and 7720 seconds in F814W, with 14 and 16 frames of differing individual exposure times in the two data-groups respectively. The cluster Fornax 4 was observed in program 5637 and has somewhat more limited data – total exposure times of 2400 seconds in both filters, and only 3 frames per data-group. Again, the individual frames have varying exposure durations. These are fully described in the notes to Table 1.

The four Sagittarius dSph globular clusters have only been targeted by one *HST* WFPC2 program – number 6701. Again, the observations were made using the F555W and F814W filters. For these four clusters (again as described in Section 3) we only required one frame in each colour – we selected those of exposure duration 300 seconds (except for Terzan 8 through the F814W filter, for which only a 260 second exposure was usable). There were no significantly shorter or longer exposures available in the archive.

Finally, it is worth noting that it has recently been plausibly demonstrated that the young outer halo globular cluster Palomar 12 is a former member of the Sagittarius dwarf, taking its census of clusters to five (Martínez-Delgado et al. 2002; Dinescu et al. 2000). Unfortunately, Pal 12 has not been observed by *HST* and therefore could not be added to the present study.

2.2 Literature data

In the interests of presenting a detailed study of the two dSph cluster systems, we have compiled literature data for the positions, ages, metallicities, distances, and reddenings of all nine clusters. The position, age, and metallicity data are presented in Table 3, and the distance and reddening data in Table 4. Like the literature compilations in Papers I and II, this tabulation is not intended to be an exhaustive study of the entire available literature – its purpose is rather to provide a consistent set of measurements for use in this and future work.

2.2.1 Cluster names and positions

We have taken the most common names for the nine clusters from the Simbad Astronomical Database (<http://simbad.u-strasbg.fr/>). The Fornax clusters are labelled as Fornax 1 – 5, according to the notation of Hodge (1961). Cluster Fornax 3 also has an NGC designation – it is NGC 1049. M54 is the brightest of the Sagittarius clusters, and is also known as NGC 6715. The remaining three clusters are of significantly lower surface density and do not have NGC entries. The names of clusters Terzan 7 and Terzan 8 refer to the catalogue of Terzan (1968), while that for cluster Arp 2 refers to the list by Arp (1965).

All positions are also taken from Simbad. For the Sagittarius clusters, these positions correspond to those presented by Harris (1996) (1999 update). Using these positions we calculated the angular separations R_{ang} of the clusters from the centres of their respective parent galaxies. For the Fornax dSph we adopted the optical centre from Simbad, at $\alpha = 02^h 39^m 59^s.3$, $\delta = -34^\circ 26' 57''$

Table 1. Observation details for the Fornax dSph globular clusters.

Cluster Name	Program ID	Principal Frames ^{a,b}					Secondary Frames ^{a,b}				
		Filter	Data-group	Date	N_e	Time (s)	Filter	Data-group	Date	N_e	Time (s)
Fornax 1	5917	F555W	u30m010eb	04/06/1996	14	5640	F814W	u30m010ib	04/06/1996	16	7720
Fornax 2	5917	F555W	u30m020eb	06/06/1996	14	5640	F814W	u30m020ib	06/06/1996	16	7720
Fornax 3	5917	F555W	u30m030eb	05/06/1996	14	5518	F814W	u30m030ib	05/06/1996	16	7720
Fornax 4	5637	F555W	u2lb0205b	10/03/1995	3	2400	F814W	u2lb0203b	10/03/1995	3	2400
Fornax 5	5917	F555W	u30m040eb	04/06/1996	14	5640	F814W	u30m040ib	04/06/1996	16	7720

^a N_e is the total number of useful frames in the listed data-group. The F555W data-group for Fornax 3 has one exposure which is shorter than was intended (378s instead of 500s; see below).

^b The column labelled “Time” shows the total exposure time for a given data-group – that is, the sum of the exposure times for each of the N_e useful frames in that data-group. Not all frames had equal individual exposure times. The combinations are as follows: (a) Fornax 1, Fornax 2, & Fornax 5: F555W = $3 \times 600s$, $4 \times 500s$, $3 \times 400s$, $4 \times 160s$; F814W = $2 \times 900s$, $6 \times 700s$, $2 \times 500s$, $6 \times 120s$; (b) Fornax 3: F555W = $3 \times 600s$, $3 \times 500s$, $3 \times 400s$, $1 \times 378s$, $4 \times 160s$; F814W = $2 \times 900s$, $6 \times 700s$, $2 \times 500s$, $6 \times 120s$; (c) Fornax 4: F555W = $2 \times 1100s$, $1 \times 200s$; F814W = $2 \times 1100s$, $1 \times 200s$.

Table 2. Observation details for the Sagittarius dSph globular clusters.

Cluster Name	Program ID	Principal Frame				Secondary Frame			
		Filter	Data set	Date	Time (s)	Filter	Data set	Date	Time (s)
M54	6701	F555W	u37ga409r	30/08/1999	300	F814W	u37ga401r	30/08/1999	300
Terzan 7	6701	F555W	u37g020br	18/03/1997	300	F814W	u37g0202r	18/03/1997	300
Terzan 8	6701	F555W	u37g1307r	26/03/1999	300	F814W	u37g1306r	26/03/1999	260
Arp 2	6701	F555W	u37g0107m	11/05/1997	300	F814W	u37g0101m	11/05/1997	300

(J2000.0) – this is consistent with the centroids derived by Demers et al. (1994), and Irwin & Hatzidimitriou (1995). For the Sagittarius dSph, it is difficult to define an optical centre because of the severely disrupted nature of the galaxy. We have adopted the centre to be the location of the densest clump of stars, upon which M54 is exactly superposed (Ibata et al. 1994; Ibata et al. 1997), at $\alpha = 18^h 55^m 03^s.28$, $\delta = -30^\circ 28' 42''.6$ (J2000.0) – indeed, it has been suggested (e.g., Layden & Sarajedini (2000)) that Sagittarius is a nucleated dwarf with M54 as its nucleus. Using R_{ang} and the distances from Table 4, we have also calculated R_{lin} – the linear separation of a given cluster from the centre of its parent galaxy. Because we have individual distance moduli for the Sagittarius clusters (Table 4), these calculations naturally account for the line-of-sight depth of this system.

2.2.2 Cluster ages

As far as we are aware, the only available studies concerning the relative ages of the Fornax globular clusters are those by Buonanno and collaborators (Buonanno et al. 1998b, 1999), who use the same *HST* images from Table 1 to construct colour magnitude diagrams (CMDs) from which they derive relative ages and metallicities for the clusters. Clusters 1, 2, 3, and 5 appear coeval with the oldest Galactic globulars, and we adopt absolute ages of 14.6 ± 1.0 Gyr (for consistency with the oldest Sagittarius clusters – see below). Cluster 4 is ~ 3 Gyr younger, and we adopt an absolute age of 11.6 ± 1.0 Gyr.

The Sagittarius clusters are more extensively studied. Layden & Sarajedini (2000) have calculated relative and absolute ages for each, and we adopt their ages for M54 and Terzan 8 in particular, as 14.7 ± 0.5 Gyr and 14.5 ± 0.8 Gyr respectively. They show these

clusters to be coeval with typical Galactic globulars of comparable metallicity (e.g., M92 and M5). We therefore used these two ages to estimate absolute ages for Fornax clusters 1, 2, 3, and 5, as listed above. We note that our adopted age for Terzan 8 is consistent with the work of Montegriffo et al. (1998), who also find this cluster to be coeval with typical metal-poor Galactic globular clusters.

Terzan 7 and Arp 2 appear younger than Terzan 8 and M54, and there are several bodies of work concerning these two clusters. For Arp 2 we directly average the results of Buonanno (1998a) (who derive an age of -1.6 ± 1.6 Gyr relative to the oldest globular clusters – i.e., in this case M54 and Terzan 8), Layden & Sarajedini (2000) (13.1 ± 0.9 Gyr), and Salaris & Weiss (2002) (11.5 ± 1.4 Gyr), which are all in good agreement, to obtain 12.5 ± 1.0 Gyr. Montegriffo et al. (1998) find an age of -4.4 ± 2.0 Gyr relative to Terzan 8, and we have not included this significantly younger age in the average. For Terzan 7 however, all four studies obtain consistent age estimates – respectively, -7.6 ± 1.7 Gyr relative to the oldest Galactic clusters; 8.3 ± 1.8 Gyr; 7.5 ± 1.4 Gyr; and -6.9 ± 2.0 Gyr relative to Terzan 8. We directly average these results to obtain an age estimate of 7.6 ± 1.0 Gyr for Terzan 7 – one of the youngest globular clusters.

2.2.3 Cluster metallicities

There are several estimates of metallicity per cluster available in the literature. For the Fornax clusters, mostly these are photometric estimates from CMDs. For consistency, we have adopted the results of the highest resolution CMD studies – those of Buonanno et al. (1998b; 1999). These are in good agreement with other previous photometric measurements for Fornax 1, 2, 3, and 5 (e.g., Buonanno et al. (1985); Demers et al. (1990); Beauchamp et al.

Table 3. Literature nomenclature, position, age and metallicity data for the cluster sample.

Principal Name ^a	Position (J2000.0)		R_{ang} ($^{\circ}$) ^b	R_{lin} (kpc) ^c	τ (Gyr)	$\log \tau$ (yr)	Age ^d References	Metallicity [Fe/H]	Metallicity ^d References
Fornax 1	02 ^h 37 ^m 02 ^s .1	−34°11′00″	0.67	1.60	14.6 ± 1.0	10.16 ± 0.03	6	−2.20 ± 0.20	6 (2, 9, 12)
Fornax 2	02 ^h 38 ^m 40 ^s .1	−34°48′05″	0.44	1.05	14.6 ± 1.0	10.16 ± 0.03	6	−1.78 ± 0.20	6 (1, 2)
Fornax 3	02 ^h 39 ^m 52 ^s .5	−34°16′08″	0.18	0.43	14.6 ± 1.0	10.16 ± 0.03	6	−1.96 ± 0.20	6 (2, 10, 12)
Fornax 4	02 ^h 40 ^m 09 ^s	−34°32′24″	0.10	0.24	11.6 ± 1.0	10.06 ± 0.04	7	−1.9 ± 0.2	7 (1, 10)
Fornax 5	02 ^h 42 ^m 21 ^s .15	−34°06′04″.7	0.60	1.43	14.6 ± 1.0	10.16 ± 0.03	6	−2.20 ± 0.20	6 (2, 10)
M54	18 ^h 55 ^m 03 ^s .28	−30°28′42″.6	0.00	0.00	14.7 ± 0.5	10.17 ± 0.02	13	−1.79 ± 0.08	17 (8, 11, 19)
Terzan 7	19 ^h 17 ^m 43 ^s .7	−34°39′27″	6.26	4.85	7.6 ± 1.0	9.88 ^{+0.05} _{−0.06}	5, 13, 14, 16	−0.82 ± 0.15	18 (3, 8, 11)
Terzan 8	19 ^h 41 ^m 45 ^s .0	−34°00′01″	10.30	4.92	14.5 ± 0.8	10.16 ^{+0.02} _{−0.03}	13 (14)	−1.99 ± 0.08	8 (14, 15)
Arp 2	19 ^h 28 ^m 44 ^s .1	−30°21′14″	7.27	3.80	12.5 ± 1.0	10.10 ^{+0.03} _{−0.04}	5, 13, 16 (14)	−1.84 ± 0.09	18 (4, 8, 11)

Reference list (see also text): 1. Beauchamp et al. (1995); 2. Buonanno et al. (1985); 3. Buonanno et al. (1995a); 4. Buonanno et al. (1995b); 5. Buonanno et al. (1998a); 6. Buonanno et al. (1998b); 7. Buonanno et al. (1999); 8. Da Costa & Armandroff (1995); 9. Demers et al. (1990); 10. Dubath et al. (1992); 11. Harris (1996) (1999 update); 12. Jørgensen & Jimenez (1997); 13. Layden & Sarajedini (2000); 14. Montegriffo et al. (1998); 15. Ortolani & Gratton (1990); 16. Salaris & Weiss (2002); 17. Sarajedini & Layden (1995); 18. Sarajedini & Layden (1997); 19. Zinn & West (1984).

^a Fornax 3 is also known as NGC 1049, while M54 is also known as NGC 6715.

^b Angular separation relative to the optical centre of (a) the Fornax dSph, at $\alpha = 02^h39^m59^s.3$, $\delta = -34^{\circ}26'57''$ (J2000.0) (Simbad Astronomical Database, see also Demers et al. (1994); Irwin & Hatzidimitriou (1995)); (b) the Sagittarius dSph, taken to be the position of M54 (see e.g., Layden & Sarajedini (2000); Ibata et al. (1997); Ibata et al. (1994)).

^c Estimated linear separations to the optical centres of either the Fornax or Sagittarius dwarfs, calculated from R_{ang} and the cluster distance moduli from Table 4. We assume the distance to the centre of the Fornax dSph to be ~ 137 kpc (Buonanno et al. 1999), and that for the Sagittarius dSph to be equivalent to the M54 distance from Harris (1996).

^d Principal references (i.e., for the adopted metallicity or age value) are given first. In some cases these are followed by references in parenthesis, which show literature complementary to the principal reference, as described in the text. Entries with multiple non-bracketed references indicate that an average of the individual values from these respective sources has been adopted, again as described in the text.

(1995); Jørgensen & Jimenez (1997)). Dubath, Meylan & Mayor (1992) provide spectroscopic metallicity determinations for Fornax 3, 4, and 5. Again, those for Fornax 3 and 5 are in good agreement with the photometric estimates. Cluster 4 however, shows a discrepancy between the photometric metallicity determinations (Beauchamp et al. 1995; Buonanno et al. 1999) and those derived from spectroscopy (Dubath et al. 1992; Beauchamp et al. 1995) – the measurements are $[\text{Fe}/\text{H}] \sim -1.9$ and $[\text{Fe}/\text{H}] \sim -1.3$ respectively. Cluster 4 is in a relatively dense region of the Fornax dwarf, and it is possible that field stars (which are measured to have $[\text{Fe}/\text{H}] \sim -1.3$) have contaminated the spectroscopic measurements. However, Buonanno et al (1999) note that a similar discrepancy is well known for several Galactic clusters – in particular Rup 106 and Pal 12 – and that it may be linked to the fact that these clusters appear to be $[\alpha/\text{Fe}]$ -deficient relative to other globular clusters (see also Sarajedini & Layden (1997) for a detailed discussion). It might be that Fornax 4 is a similar case.

Interestingly, the (young) Sagittarius clusters Terzan 7 and Arp 2 show a similar discrepancy between their photometrically and spectroscopically determined metallicities. For Terzan 7, the CMD study of Sarajedini & Layden (1997) measured $[\text{Fe}/\text{H}] = -0.82 \pm 0.15$, which is consistent with the study of Buonanno et al. (1995a). However, Da Costa & Armandroff (1995) obtained $[\text{Fe}/\text{H}] = -0.36 \pm 0.09$ from spectroscopy of the Ca II triplet. Similarly, for Arp 2 Sarajedini & Layden (1997) measured $[\text{Fe}/\text{H}] = -1.84 \pm 0.09$ (in good agreement with Buonanno et al. (1995b)) while Da Costa & Armandroff (1995) observed $[\text{Fe}/\text{H}] = -1.70 \pm 0.11$. These discrepancies are in the same sense as those for Fornax 4, Rup 106, and Pal 12 – namely that the spectroscopic measurements suggest higher metallicities than are consistent with

the clusters' CMDs. For the present, we adopt, for internal consistency, the photometrically determined values; further observations will no doubt clarify the situation in the near future. We feel that it is worth noting that all of the clusters which show this discrepancy are conclusively linked with local dwarf galaxies, except Rup 106. It would be worthwhile searching in the vicinity of this cluster for any evidence of debris from a former parent galaxy, such as that found surrounding Pal 12 by Martínez-Delgado et al. (2002).

Metallicity determinations for Terzan 8 are much simpler to interpret. There is good agreement between the spectroscopic measurements by Da Costa & Armandroff (1995) and the photometric estimates of Montegriffo et al. (1998) and Ortolani & Gratton (1990). For M54, again there appears a discrepancy between the photometric measurement of Sarajedini & Layden (1995) and the spectroscopy of Da Costa & Armandroff (1995). However, like for the massive globular cluster ω Cen, Sarajedini & Layden (1995) have suggested that M54 may possess an internal metallicity dispersion, of $\sigma([\text{Fe}/\text{H}]) = 0.16$ dex. Da Costa & Armandroff conclude that if this is indeed the case then the two measurements are consistent. As with the other clusters, we adopt the photometric determination.

2.2.4 Distances and reddenings

Accurate distances are necessary for converting measured parameters from observational to physical units (e.g., arcseconds to parsecs), as well as for estimating total cluster luminosities – a task for which we also require accurate reddenings. Since both calculations were desirable for this study (see Section 4), we also compiled distance and reddening data from the literature, as listed in Table 4.

Table 4. Literature distance and reddening data for the cluster sample.

Cluster	Distance Modulus ^a	Reference ^b	Distance (kpc)	Scale Factor (arcsec pc ⁻¹)	$E(B - V)^c$	$E(V - I)^c$	Reference ^b
Fornax 1	20.68 ± 0.20	7	$137 (\pm 13)$	$1.508 (\pm 0.144)$	(0.04 ± 0.05)	0.05 ± 0.06	6
Fornax 2	20.68 ± 0.20	7	$137 (\pm 13)$	$1.508 (\pm 0.144)$	(0.07 ± 0.05)	0.09 ± 0.06	6
Fornax 3	20.68 ± 0.20	7	$137 (\pm 13)$	$1.508 (\pm 0.144)$	(0.04 ± 0.05)	0.05 ± 0.06	6
Fornax 4	20.68 ± 0.20	7	$137 (\pm 13)$	$1.508 (\pm 0.144)$	(0.12 ± 0.05)	0.15 ± 0.06	7
Fornax 5	20.68 ± 0.20	7	$137 (\pm 13)$	$1.508 (\pm 0.144)$	(0.06 ± 0.05)	0.08 ± 0.06	6
M54	17.17 ± 0.15	11	$27.2 (\pm 1.9)$	$7.583 (\pm 0.532)$	(0.14 ± 0.02)	0.18 ± 0.02	13
Terzan 7	16.83 ± 0.15	11	$23.2 (\pm 1.6)$	$8.891 (\pm 0.616)$	0.07 ± 0.03	(0.09 ± 0.04)	18
Terzan 8	17.08 ± 0.15	11	$26.0 (\pm 1.8)$	$7.933 (\pm 0.552)$	0.12 ± 0.03	(0.15 ± 0.04)	14
Arp 2	17.28 ± 0.15	11	$28.6 (\pm 2.0)$	$7.212 (\pm 0.507)$	0.10 ± 0.02	(0.13 ± 0.03)	18

^a Dereddened visual distance modulus. For the Sagittarius clusters, we have taken the apparent distance moduli of Harris (1996) and corrected these using the reddenings of columns 6 & 7 and the extinction laws described in Section 2.2.4.

^b Numbers refer to entries in the Reference list at the end of Table 3.

^c Values in parenthesis have been calculated from the neighbouring column using the extinction laws described in Section 2.2.4.

For the Fornax clusters, we adopted a single (dereddened) distance modulus of 20.68 ± 0.20 , as suggested from the extensive discussion of Buonanno et al. (1999). This corresponds to a distance of 137 ± 13 kpc, consistent with other literature measurements (e.g., Buonanno et al. (1985); Demers et al. (1990)). The high resolution CMD studies of Buonanno and collaborators (Buonanno et al. 1998b; Buonanno et al. 1999) also provide $E(V - I)$ colour excesses, as listed in Table 4.

For completeness, we would like to include estimates of the $E(B - V)$ colour excesses for these clusters. This requires some knowledge of interstellar extinction laws, which are also required for calculating dereddened distance moduli for the Sagittarius clusters (see below). We take the definition of the colour excess as $E(\lambda_1 - \lambda_2) = A_{\lambda_1} - A_{\lambda_2}$, where λ_1 and λ_2 are the passbands being considered, and the A_λ values are the extinctions in these passbands. Following Cardelli, Clayton & Mathis (1989), we can also define $c = A_{\lambda_2}/A_{\lambda_1}$, which means that in our present case (where V and I are our two passbands) we have $A_V = (1 - c)^{-1}E(V - I)$. Interpolating in Table 3 of Cardelli, Clayton & Mathis (1989), we find that $c \sim 0.578$, assuming that the centre of the I passband is 814 nm. Therefore, we obtain $A_V = 2.37E(V - I)$. Cardelli et al. make the assumption that $A_V = 3.1E(B - V)$, which implies that $E(V - I) = 1.31E(B - V)$. These relations allow us to compute reddenings and colour excesses as appropriate – this is also important in the luminosity calculations of Section 4.2.

For the Sagittarius clusters, we adopt the individual apparent distance moduli from Harris (1996) (1999 update), and have dereddened them using the quoted colour excesses (also listed by Harris) and the extinction laws described above to obtain the values in Table 4. The original references for the colour excesses (all determined from high data-quality CMD studies) are as follows: M54, Layden & Sarajedini (2000); Terzan 8, Montegriffo et al. (1998); Terzan 7 and Arp 2, Sarajedini & Layden (1997).

3 PHOTOMETRY AND SURFACE BRIGHTNESS PROFILES

The data reduction, photometry, and construction of surface brightness profiles followed almost exactly the procedures outlined in Papers I and II for the Magellanic Cloud clusters, and for a detailed

description we refer the reader to these. However, the Fornax and Sagittarius globular clusters, at respectively twice and half the distances of the Magellanic clusters, presented their own set of challenges, and in several places we altered the reduction procedure. For continuity, we therefore provide a brief summary of the overall reduction process below, and describe the details of the changes made to the procedure of Papers I and II where applicable.

The first alteration came at the very start of the reduction process, during the image preparation. As described in Papers I and II, for the old ($\tau \sim 10^{10}$ yr) Magellanic Cloud clusters, it had generally been sufficient to use one frame of several hundred seconds' exposure time, in each of two colours per cluster, to obtain the photometry for use in constructing the surface brightness profiles. For the Sagittarius clusters, this was again sufficient. The Fornax clusters however, are more than twice as distant as the Magellanic Cloud clusters, and therefore appear considerably fainter and more crowded. For these clusters, it was necessary to take many frames per colour per cluster (Table 1), and stack them together to obtain suitable photometry.

The data were first retrieved from the *HST* archive. As part of the retrieval process, all exposures are reduced according to the standard WFPC2 pipeline, using the latest available calibrations. This ensures that all the data has been treated using the calibration from a single epoch, and with the longest baseline. To obtain photometry from these reduced frames, we used the HSTphot software of Dolphin (2000a), which is specifically tailored to measuring WFPC2 images. First, we pre-treated each image with the HSTphot preparation software, as described in Papers I and II. The Sagittarius data consisted of two frames (one F555W and one F814W) per cluster (see Table 2). On each frame, bad regions and pixels were masked using the STScI data quality images, cosmic rays were removed using a HSTphot routine based on the IRAF task CRREJ, potential hot-pixels were removed using a σ -clipping algorithm, and a background image was prepared.

The Fornax data were more complicated, consisting of two data-groups (one F555W and one F814W) of multiple frames per cluster. On each frame, bad regions and pixels were masked using the STScI data quality images, as usual. However, next the procedure deviated from that described in Papers I and II. First, we aligned all the frames in a specific data-group using the IRAF task IMALIGN. This routine takes a base image and treats each of the

other frames as being offset from this base by a simple linear x - and y -shift. This was perfectly suitable for the present data – all frames in a specific data-group were imaged one after the other, and any offsets were due to a deliberate dithering pattern of several pixels in x and/or y . There were no significant rotations or higher order distortions between observations which needed to be accounted for. Once registered, all the frames from a data-group were added together using the HSTphot routine *crclean*. This routine cleans cosmic rays (again using an algorithm similar to CRREJ), then adds together the counts for a given pixel in all images and scales for the total exposure time. This means that images of multiple exposure times can be combined, with the resultant “master” frame having a much higher saturation level than any of the individual images, and an effective exposure time which is the sum of that for the individual images. For each colour for each cluster, we therefore added long duration exposures to short duration exposures and the resultant image had a very low faint limit but did not suffer badly from crowding (except in the most central regions of Fornax 3, 4, and 5). This process thereby mostly alleviated the two major problems caused by the large distance of the Fornax clusters.

We then cleaned each master frame with the hot-pixel algorithm and determined a background image, just as in the usual procedure. From this point on, the two master frames for a Fornax cluster were treated exactly as the two individual frames for the clusters described in Papers I and II and the Sagittarius clusters.

Photometric measurements were made using the HSTphot module *multiphot* in PSF fitting mode, with a minimum detection threshold of 3σ above the local background. This routine aligns and solves the two (different colour) frames for a cluster simultaneously, which eliminates the need for correlating and matching between object lists, and is useful for keeping the photometry clean of spurious (e.g., cosmic ray) detections – only objects found in both frames were kept. Parameters derived from the PSF fitting, such as the object classification, sharpness, and goodness-of-fit were used as described in Papers I and II to further clean the detection list of spurious and non-stellar objects. Photometry in both colours for the selected objects was corrected for geometric distortion, any filter-dependent plate scale changes, and the WFPC2 34th row defects and charge transfer inefficiency (using the calibration of Dolphin (2000b)). Any PSF residuals were accounted for and the final photometry corrected to a $0''.5$ aperture and the zero-points of Dolphin (2000b).

With the photometry complete, for each cluster we calculated positions for all stars in corrected pixel coordinates (pixel coordinates corrected for geometric distortion and relative to the WFC2 origin) using the IRAF STSDAS task METRIC. We then determined the position of the cluster’s central surface brightness peak, using the random sampling algorithm described in Paper I. This centering is performed using the photometry in both colours (a good consistency check) and is typically repeatable to ± 10 WFC pixels, or approximately ± 1 second of arc.

In each colour, we measured the cluster’s surface brightness profile via radial binning about the calculated centre. For each cluster, four different sets of annuli were generated. In the case of the Fornax clusters and M54, two sets were of narrow ($1.5''$ and $2''$) width and extended to $\sim 20''$ and $\sim 30''$ respectively, while the remaining two sets were wider ($3''$ and $4''$) and extended as far as possible (typically $\sim 80''$). This is just as described for the Magellanic Cloud clusters in Papers I and II. For the Sagittarius clusters Terzan 7, Terzan 8, and Arp 2 however, the annulus widths had to be adjusted. These three clusters are intrinsically sparse (see Table 5), and combined with their relatively close distance (~ 25 kpc) and

the small WFPC2 field of view, this means that the stellar density in the observed frames is very low. These three clusters therefore required significantly wider annuli to obtain useful profiles. A small amount of experimentation resulted in the following widths: Terzan 7 – $2''$, $3''$, $4''$, and $6''$; Terzan 8 – $7''$, $8''$, $9''$, and $10''$; Arp 2 – $8''$, $9''$, $10''$, and $11''$.

We calculated the surface brightness μ_i of the i -th annulus in a given annulus set by summing the flux of all stars contained in that annulus:

$$\mu_i = \frac{A_i}{\pi(b_i^2 - a_i^2)} \sum_{j=1}^{N_s} C_j F_j \quad (1)$$

where a_i and b_i are respectively the inner and outer radii of the annulus, N_s is the number of stars in the annulus, F_j is the flux of the j -th star, and the coefficients A_i and C_j are correction factors for the annulus area and the detection completeness respectively. The area correction factors arise because most annuli are not fully “imaged” by the WFPC2 field of view, as described in Paper I. Therefore the effective area $\pi A_i^{-1}(b_i^2 - a_i^2)$ must be used in calculating the surface brightness of the annulus, rather than the full area. Because of the complicated geometry of the WFPC2 camera, and the arbitrary cluster centering and observation roll-angle, the coefficients A_i were computed numerically rather than analytically. To avoid large random uncertainties, annuli with $A_i > 4$ were not used – this determined the maximum extent r_m of each surface brightness profile. In general, $r_m \sim 75''$.

The completeness correction factors are necessary because in crowded fields such as those in globular clusters, detection software cannot find every star all the time. This results in missing flux, which should be accounted for when calculating the surface brightness in each annulus. As described in Paper I, we derived the coefficients C_j by means of artificial star tests. Fake stars were added by *multiphot* one at a time to each frame and then solved, with the output filtered according to the detection parameters, just as for the real photometry. By fully sampling an artificial CMD, for a given cluster the completeness was generated as a function of position on the camera, and stellar brightness and colour, in the form of a look-up table. For the j -th star in an annulus the appropriate C_j was located in this table, and the completeness corrected stellar flux $C_j F_j$ added to the sum. We discarded stars with $C_j > 4$ to avoid introducing large random errors – in effect, this determined the faint limit as a function of position within the cluster.

Because of the use of both short and long exposures in constructing the Fornax clusters’ master frames, none of them suffered significant saturation or crowding, except in the central-most few arcseconds in the compact Fornax clusters 3, 4, and 5. Apart from M54, none of the Sagittarius clusters suffered from crowding either – as discussed previously, these three clusters are sparsely populated, especially Terzan 8 and Arp 2. However, as with the low density old LMC clusters (e.g., NGC 1466, NGC 2210, NGC 2257) the three low density Sagittarius clusters had a smattering of saturated stars (giant branch and horizontal branch members) which were not measured by *multiphot* and which did not contribute to their respective profiles. As discussed in Paper I, we were comfortable in neglecting these stars from the calculations, because in doing so we constructed less noisy profiles without compromising the measurement of structural parameters (see also e.g., Elson et al. (1989); Elson (1991); Elson (1992)).

M54 however, is the one of the most luminous local globular clusters (e.g., Sarajedini & Layden (1995)) and is very compact. The images of this cluster therefore suffered from severe saturation

and crowding over much of the PC chip, on which M54 was centered. In Paper I, we described our technique of adding photometry from a short exposure to alleviate such problems; however, unfortunately no such short exposures are available in the *HST* archive for M54. This meant we were unable to extend the profile for this cluster within approximately $7''$. As with the compact old clusters in the LMC bar (e.g., NGC 1754, NGC 1786, NGC 2005, etc) there were also a number of saturated (giant) stars outside the central region of the cluster – again, as described above, it was acceptable to neglect these stars from the profile calculations.

For the three Fornax clusters which were saturated and crowded within $\sim 5''$ radius, we were able to use photometry from individual aligned short exposures (see Table 1) from the respective data-groups to construct complete profiles, exactly following the procedure described in Paper I.

For every annulus, the uncertainty σ_i in the surface brightness was initially calculated by dividing the annulus into eight segments, and evaluating the standard deviation of the surface brightnesses of the segments. This technique proved unsuitable for the outer regions of many clusters however, significantly underestimating the point-to-point scatter. To account for this, after the background subtraction (see below) on a profile, we calculated the Poisson error for each annulus, and in cases where this was significantly larger than the segmental error, we adopted the new uncertainty in preference. As a consequence of this technique, for some profiles the errors appear larger than the RMS point-to-point scatter. For a full discussion of this, and the error calculation procedure in general, we refer the interested reader to Paper I.

We next fit models to each measured profile. For Magellanic clusters, we found the most suitable models to be those of Elson, Fall & Freeman (1987) (hereafter EFF models), which have the form:

$$\mu(r) = \mu_0 \left(1 + \frac{r^2}{a^2} \right)^{-\frac{\gamma}{2}} \quad (2)$$

where μ_0 is the central surface brightness, a is a measure of the scale length and γ is the power-law slope at large radii. This is essentially an empirical King (1962) model, without the tidal truncation – because of the WFPC2 field of view, no profiles of Magellanic Cloud clusters were ever measured to their tidal radii. Clearly, for the Sagittarius clusters (much closer than the Magellanic Cloud clusters) such models were again sufficient. For the Fornax clusters however, previous measurements (see e.g., Webbink (1985); Demers, Kunkel & Grondin (1990); Demers, Irwin & Kunkel (1994); Rodgers & Roberts (1994); Smith et al. (1996)) suggested tidal radii in the range $\sim 50'' - 120''$, so it seemed possible that we *would* measure to the tidal limits of some clusters. Ultimately however, we did not observe any apparent cut-offs (see Section 4.1.1) and EFF profiles again proved sufficient.

The traditional King core radius r_c is related to the EFF scale length a by the relation:

$$r_c = a(2^{2/\gamma} - 1)^{1/2} \quad (3)$$

provided the tidal cut-off $r_t \gg r_c$ – a safe assumption for all the clusters measured here.

The best fitting EFF profiles were determined via weighted least-squares minimization; again for a full discussion, we refer the reader to Paper I. As part of the fitting process, we estimated a background level (due to field stars) for each cluster. Because separate offset background images were not available, this was achieved by first fitting a model only to the very centre of a given cluster profile (bright enough to be effectively free of background contamina-

tion), to obtain estimates for μ_0 and r_c . These were then used to fit a model of the form $r^{-\gamma} + \phi$ to the outer part of the profile, where ϕ is the (constant) background level. We then subtracted this level from the whole profile, calculated the Poisson error for each annulus (as described above), and fit an EFF model to the entire background subtracted profile to obtain final measures of (μ_0, γ, a) . Uncertainties in these parameters were determined via a bootstrap algorithm, with 1000 iterations (see e.g., Press et al. (1992), p. 691). We have previously verified that this subtraction and fitting procedure does not introduce any large systematic errors into the measured values of γ – the parameter most sensitive to the assumed background contamination.

Finally, we note that while profiles and parameter measurements are presented here for only the F555W photometry[†], similar profiles and measurements exist for the F814W photometry (much as secondary profiles exist in F450W or F814W for the LMC and SMC clusters in Papers I and II). These measurements provide a good consistency check on the F555W profiles and parameters and also offer the opportunity for studies of colour profiles, for example. The second colour measurements *are* available on-line, as described in Section 1.

4 RESULTS

4.1 Profiles and structural parameters

The background-subtracted F555W surface brightness profiles for the Fornax dwarf globular clusters are presented in Fig. 1, and those for the Sagittarius dwarf globular clusters in Fig. 2. The results of the EFF model fitting are listed in Table 5. Because of the limiting resolution of our profiles (set by the smallest annulus width), the measurements of r_c for the compact clusters Fornax 3, 4, and 5 are best considered as upper limits.

4.1.1 Comparison with previous work

It is worthwhile comparing our results with those from previously published studies. The structures of the Fornax clusters have been measured by Demers, Kunkel & Grondin (1990) (Fornax 1); Demers, Irwin & Kunkel (1994) (Fornax 2, 3, 4, 5); Rodgers & Roberts (1994) (all clusters); and Smith et al. (1996) (Fornax 1 & 5). Webbink (1985) also includes estimates of the structural parameters for all five clusters in his compilation for Galactic globular clusters. The Sagittarius clusters are less well studied – profiles are presented for M54, Terzan 7, and Arp 2 by Trager, King & Djorgovski (1995) (although the profiles for Terzan 7 and Arp 2 are of low resolution), and structural measurements by Chernoff & Djorgovski (1989). An estimate for the structural parameters of Terzan 8 is included in the compilation of Trager, Djorgovski & King (1993). Estimates for all four clusters are also provided in Webbink's (1985) collection.

The values for the structural parameters of each cluster, taken from the above publications, are displayed in Table 6, and the core radii from this table are plotted against our measured values in Fig. 3. We first consider the Fornax clusters (plotted as circles). As is evident from Table 6, for each of the five clusters there is significant scatter in the literature measurements; however, in many cases

[†] The reason for this is mainly to do with clarity – presenting a second full set of results would tend to unnecessarily extend and dilute the flow of the paper.

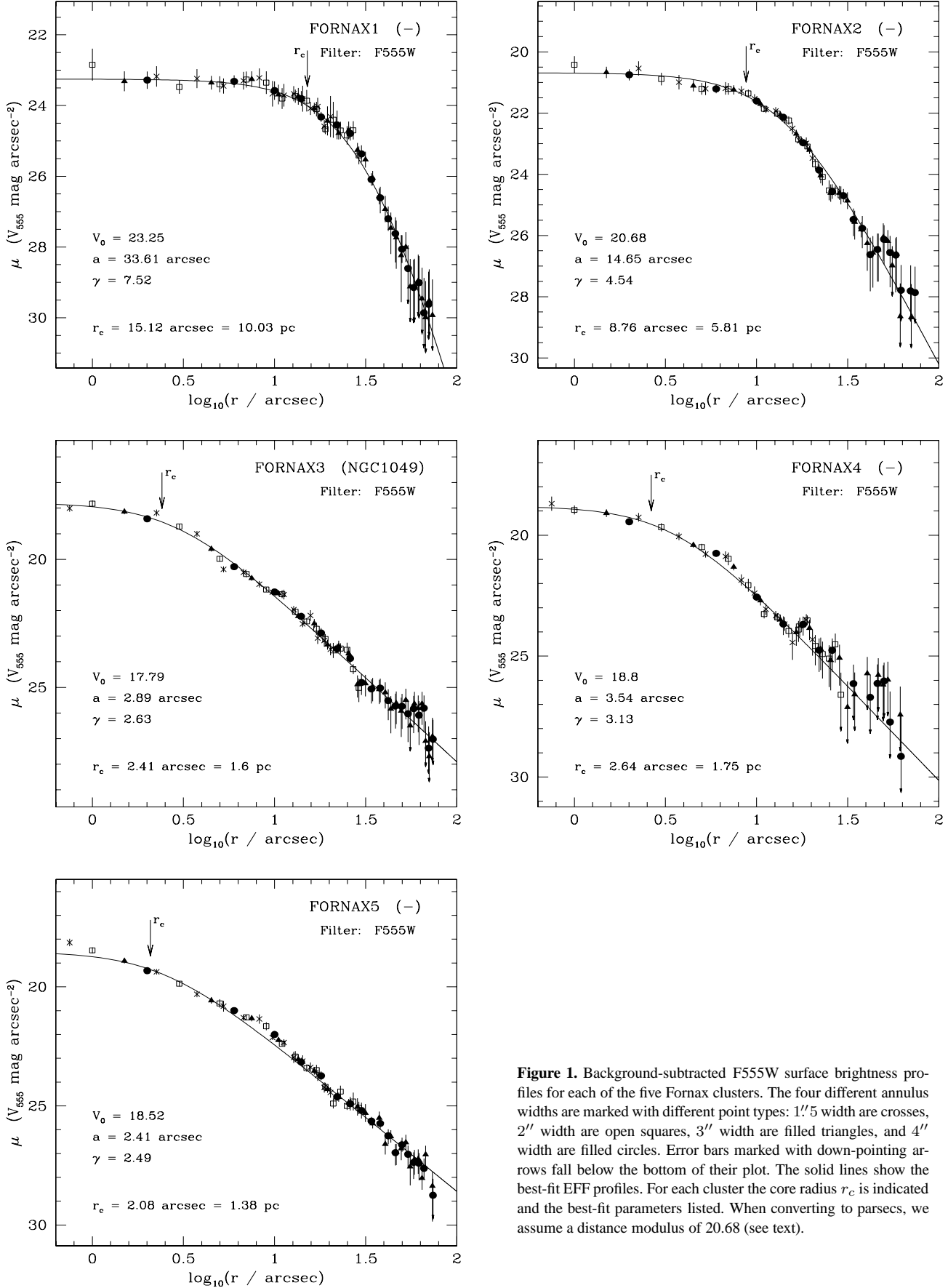


Figure 1. Background-subtracted F555W surface brightness profiles for each of the five Fornax clusters. The four different annulus widths are marked with different point types: 1''.5 width are crosses, 2'' width are open squares, 3'' width are filled triangles, and 4'' width are filled circles. Error bars marked with down-pointing arrows fall below the bottom of their plot. The solid lines show the best-fit EFF profiles. For each cluster the core radius r_c is indicated and the best-fit parameters listed. When converting to parsecs, we assume a distance modulus of 20.68 (see text).

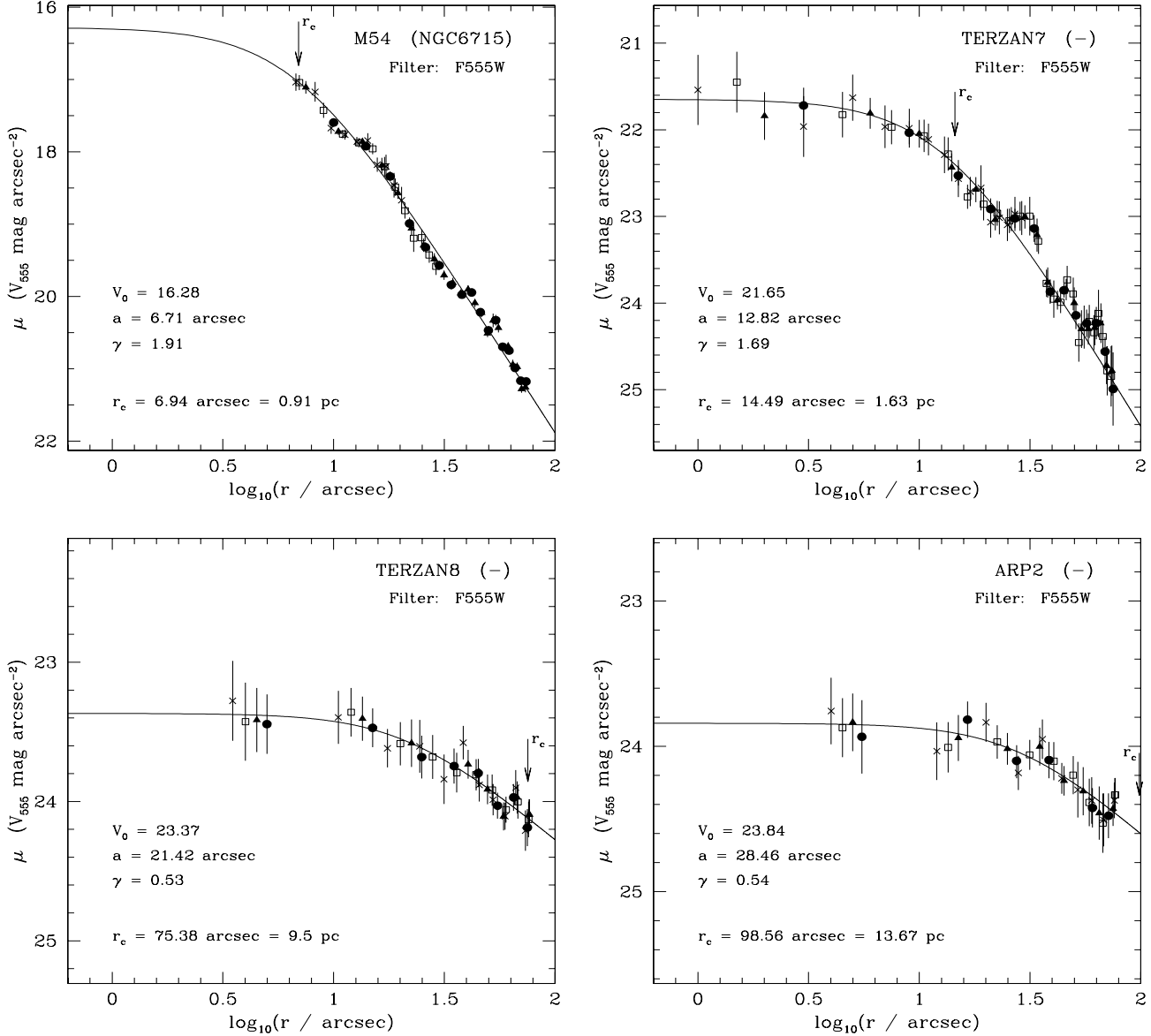


Figure 2. Background-subtracted F555W surface brightness profiles for each of the four Sagittarius clusters. For each cluster, the four different annulus widths are marked with different point types. These are (see text): M54: 1''5 (crosses), 2'' (open squares), 3'' (filled triangles), 4'' (filled circles); Terzan 7: 2'' (crosses), 3'' (open squares), 4'' (filled triangles), 6'' (filled circles); Terzan 8: 7'' (crosses), 8'' (open squares), 9'' (filled triangles), 10'' (filled circles); Arp 2: 8'' (crosses), 9'' (open squares), 10'' (filled triangles), 11'' (filled circles). Error bars marked with down-pointing arrows fall below the bottom of their plot. The solid lines show the best-fit EFF profiles. For each cluster the core radius r_c is indicated and the best-fit parameters listed. When converting to parsecs, we assume the distance moduli from Table 4.

the uncertainties are also large. In general, our agreement with previous measurements is good, and there seem to be no systematic offsets for any given cluster, or literature data set. This is consistent with any discrepancies being due to random errors – especially likely given the difficulties associated with ground-based measurements of such distant clusters. For example, many of the literature measurements for the compact clusters Fornax 3, 4, and 5 are larger than the core radii calculated in this paper. This is consistent with the seeing-limited resolution of ground-based imaging. The most discrepant measurement is that for the core radius of Fornax 1 from Rodgers & Roberts (1994); however there is a good explanation for this. Fornax 1 has a somewhat patchy appearance, and the surface

brightness profile of Rodgers & Roberts reflects this with a large bump at around 10''. Their best-fit King model does not account for this bump, and they therefore measure a smaller value for r_c than we do here. Their profile however, is also consistent with a larger r_c , similar to that from Demers et al. (1990) or Smith et al. (1996), who also show very bumpy profiles.

It is also worth considering the tidal radii for the Fornax clusters. Of the five surface brightness profiles, none shows any good evidence for a tidal turn-down in its outer regions. A comparison between the literature values for r_t and the maximum extent of our surface brightness profiles shows that it is indeed unlikely that we have measured past the tidal cut-offs of any of the clusters except

Table 5. Structural parameters for the cluster sample derived from the best-fitting F555W EFF profiles.

Cluster Name	Centre (J2000.0) ^a		$\mu_{555}(0)^b$	a ($''$)	γ	r_c ($''$)	r_c (pc) ^c	r_m ($''$)
	α	δ						
Fornax 1	02 ^h 37 ^m 01 ^s .9	−34°11′01″	23.25 ± 0.04	33.61 ± 2.42	7.52 ± 0.64	15.12 ± 0.43	10.03 ± 0.29	75
Fornax 2	02 ^h 38 ^m 44 ^s .1	−34°48′30″	20.68 ± 0.06	14.65 ± 0.84	4.54 ± 0.23	8.76 ± 0.29	5.81 ± 0.19	76
Fornax 3	02 ^h 39 ^m 48 ^s .1	−34°15′30″	17.79 ± 0.07	2.89 ± 0.17	2.63 ± 0.06	2.41 ± 0.11	1.60 ± 0.07	76
Fornax 4	02 ^h 40 ^m 07 ^s .6	−34°32′10″	18.80 ± 0.11	3.54 ± 0.47	3.13 ± 0.20	2.64 ± 0.27	1.75 ± 0.18	64
Fornax 5	02 ^h 42 ^m 21 ^s .1	−34°06′07″	18.52 ± 0.14	2.41 ± 0.24	2.49 ± 0.06	2.08 ± 0.17	1.38 ± 0.11	76
M54	18 ^h 55 ^m 03 ^s .3	−30°28′46″	16.28 ± 0.05	6.71 ± 0.40	1.91 ± 0.04	6.94 ± 0.32	0.91 ± 0.04	76
Terzan 7	19 ^h 17 ^m 43 ^s .9	−34°39′29″	21.65 ± 0.05	12.82 ± 1.23	1.69 ± 0.07	14.49 ± 1.03	1.63 ± 0.12	78
Terzan 8	19 ^h 41 ^m 45 ^s .2	−34°00′03″	23.37 ± 0.04	21.42 ± 6.14	0.53 ± 0.11	75.38 ± 5.71	9.50 ± 0.72	81
Arp 2	19 ^h 28 ^m 45 ^s .2	−30°21′21″	23.84 ± 0.04	28.46 ± 8.29	0.54 ± 0.15	98.56 ± 13.33	13.67 ± 1.85	81

^a We find our centering algorithm to be repeatable to approximately $\pm 1''$, notwithstanding image header inaccuracies. Given this precision, coordinates in δ are provided to the nearest arcsecond. Those in α are reported to the nearest tenth of a second, but the reader should bear in mind that at $\delta = -30^\circ$, one second of RA corresponds to approximately thirteen seconds of arc – in other words, the uncertainty in α is slightly smaller than ± 0.1 .

^b The V_{555} magnitude of one square arcsecond at the centre of a given cluster.

^c When converting to parsecs we assume the distance moduli and scale factors from Table 4.

Table 6. Previously published structural parameter measurements.

Cluster	r_c ($''$) (published) ^a	References	r_c ($''$) (this paper)	r_t ($''$) (published) ^b	References	r_m ($''$) (this paper)
Fornax 1	19 ± 1; 5.9 ± 0.6; 17.6; 14.4 ± 4.9	2; 5; 6; 9	15.12 ± 0.43	56 ± 5; 104; 91 ± 36	2; 6; 9	75
Fornax 2	4 ± 1; 5.5 ± 0.6; 8.7 ± 1.0	3; 5; 9	8.76 ± 0.29	74 ± 5; 114 ± 27	3; 9	76
Fornax 3	4 ± 1; 3.4 ± 0.3; 1.4 ± 0.5	3; 5; 9	2.41 ± 0.11	77 ± 5; 95 ± 22	3; 9	76
Fornax 4	7 ± 1; 3.9 ± 0.4; 1.0 ± 0.4	3; 5; 9	2.64 ± 0.27	43 ± 5; 66 ± 15	3; 9	64
Fornax 5	4 ± 1; 3.7 ± 0.4; ~ 2 (UL); 4.2 ± 1.6	3; 5; 6; 9	2.08 ± 0.17	74 ± 5; 91; 76 ± 18	3; 6; 9	76
M54	6.3 ± 1.5; 6.5 ± 1.5; 6.3 ± 0.7	1; (8, 4); 9	6.94 ± 0.32	446 ± 157; 446 ± 215; 445 ± 104	1; (8, 4); 9	76
Terzan 7	39.8 ± 9.2; 36.3 ± 17.3; 21.8 ± 8.2	1; (8, 4); 9	14.49 ± 1.03	199 ± 71; ~ 440 (OM); 209 ± 84	1; (8, 4); 9	78
Terzan 8	~ 60 (OM); 46.6 ± 17.6	(7, 4); 9	75.38 ± 5.71	~ 240 (OM); 523 ± 210	(7, 4); 9	81
Arp 2	100 ± 23.2; 95.5 ± 22.2; 119.7 ± 33.5	1; (8, 4); 9	98.56 ± 13.33	1000 ± 353; ~ 760 (OM); 337 ± 136	1; (8, 4); 9	81

Reference list: 1. Chernoff & Djorgovski (1989); 2. Demers et al. (1990); 3. Demers et al. (1994); 4. Harris (1996) (1999 update); 5. Rodgers & Roberts (1994); 6. Smith et al. (1996); 7. Trager et al. (1993); 8. Trager et al. (1995); 9. Webbink (1985).

^a Notes regarding errors in r_c : Errors are exactly as quoted by the authors for references 2, 3, & 5. For reference 1, the authors suggest errors of ~ 0.1 in $\log r_c$. For reference 6, no errors are quoted but the authors note that r_c for Fornax 5 is an upper limit – denoted (UL) above. For reference 8, no formal errors are quoted; however in reference 7, which contains mostly the same measurements, data quality flags are indicated. The authors state that clusters with data quality 1 (M54, Arp 2) have errors of ~ 0.1 in $\log r_c$, those with quality 2 (Terzan 7) have errors of twice this, and those with quality 4 (Terzan 8) are order of magnitude estimates – denoted (OM) above. We have used these errors to estimate the uncertainties as listed above. In reference 9, the author states that clusters with r_c from surface photometry (M54, Fornax 2) have errors of 0.049 in $\log r_c$ (r_c in arcmin), those from star counts (Arp 2) have errors of ~ 0.12 , and those estimated by eye (Fornax 1, 3, 4, 5, Terzan 7, 8) have errors of ~ 0.16 .

^b Notes regarding errors in r_t : Errors are exactly as quoted by the authors for references 2 & 3. For reference 1, the authors suggest errors of 0.1 – 0.2 (we assume 0.15) in $c = \log(r_t/r_c)$, which we use to estimate r_t and its uncertainty. For reference 6, no errors are quoted. For reference 8, again no errors are quoted; however in reference 7, which contains mostly the same measurements, data quality is indicated. The authors state that clusters with data quality 1 (M54) have errors of ~ 0.2 in c . For clusters with poorer data (Terzan 7, 8, Arp 2) we consider the estimates for r_t as order of magnitude (OM) only. In reference 9, the author states that clusters with r_t determined from star counts (M54) or aperture photometry (Fornax 2, 3, 4, 5) have errors of ~ 0.1 in $\log r_t$, and those estimated from angular diameter measurements (Fornax 1, Terzan 7, 8, Arp 2) have errors of ~ 0.17 .

perhaps Fornax 4. In this case however, the background level is quite high and the uncertainties intrinsic to our subtraction procedure have removed any fine detail in the outer region of this profile. We are therefore justified in our decision to fit EFF models to all our Fornax cluster profiles. Finally, we note that Rodgers & Roberts (1994) found that their profiles for Fornax clusters 3, 4, and 5 did

not show any evidence for tidal truncation but instead demonstrate that these clusters apparently possess extended haloes. Any such haloes are worthy of further attention; unfortunately however, our profiles are somewhat too limited in extent to confirm or refute their existence.

The profiles for the Sagittarius clusters also require careful

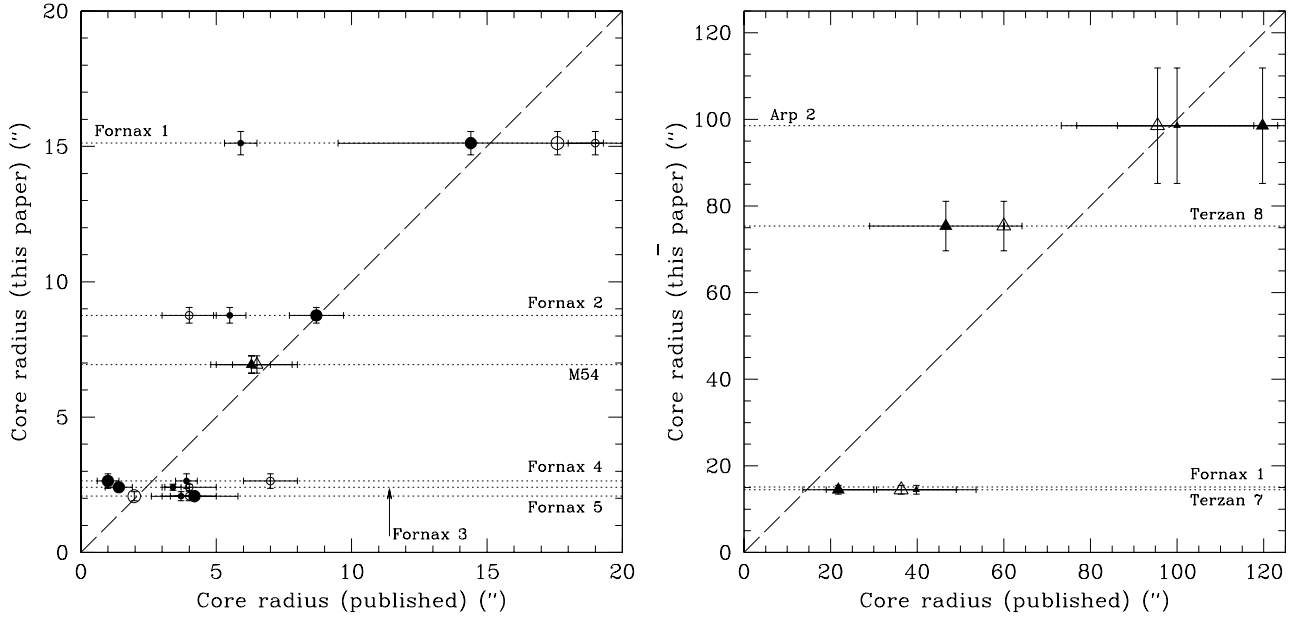


Figure 3. Measured values of r_c plotted against those previously published in the literature. *Left:* Clusters in the range $0 - 20''$. *Right:* Expanded to include clusters over the full range. In both plots, the Fornax clusters are represented by circular points and the Sagittarius clusters by triangular points. For the Fornax clusters, the literature references and corresponding point styles are: Demers et al. (1990; 1994) (small open circles); Rodgers & Roberts (1994) (small solid circles); Smith et al. (1996) (large open circles); Webbink (1985) (large solid circles). For the Sagittarius clusters, the literature references and corresponding point styles are: Chernoff & Djorgovski (1989) (small solid triangles); Trager et al. (1993; 1995) and Harris (1996) (large open triangles); Webbink (1985) (large solid triangles). On each plot, the dashed line is plotted for reference and represents equality between the measurements. The horizontal dotted lines represent the core radius measurements made in this paper, and allow the set of literature values for any given cluster to be identified. In the full-range plot, data points for the small r_c clusters have been omitted for clarity. The dotted line for Fornax 1 has been retained however, to provide some idea of the scale.

consideration. In this case, the key question is not whether the profiles have been measured too far radially, but whether they have been measured far enough. The profile for M54 is incomplete in its inner regions, while the clusters Terzan 8 and Arp 2 are so extended that their profiles are only measured to $\sim r_c$. It is therefore not clear that we are justified in considering many of our best fit parameters as good measurements for these clusters.

In particular, it is evident that for all four of the Sagittarius clusters, $\gamma < 2$. This is caused by the fact that we have measured nowhere near to the tidal limits of these clusters, as shown in Table 6. Although theoretically γ is the power-law slope of a profile at $r \gg a$, γ as determined from a best-fitting EFF model is instead the power-law slope of the measured profile *near its maximum radial extent*. Given that none of the Sagittarius clusters have been measured to near their tidal radii, it seems likely that each of the four profiles drops off much more steeply beyond r_m than our values of γ indicate, especially for Terzan 8 and Arp 2. Therefore, unlike for the Fornax clusters, where γ is a good measure of the true power-law slope at large r , we must consider our measures of γ for the Sagittarius clusters as (very) lower limits for this quantity.

It is intriguing however, that severely under-estimating γ does not seem to systematically affect our measurements of r_c for these clusters. Our value for the core radius of M54 is in good agreement with the previously published quantities, even though we are missing the inner portion of the profile and our γ is a lower limit. In addition, our measurement of $\mu_{555}(0)$ for this cluster is likely quite uncertain given that we have no inner data point to tie it down. Our value for the core radius of Terzan 7 is considerably smaller than the literature values, although is within the uncertainties for Web-

bink's (1985) measurement. We do not find cause for concern in this discrepancy – for example, the r_c of Trager et al. (1995) is measured from a low resolution profile which shows evidence of mis-centering – likely due to the ragged appearance of Terzan 7.

Terzan 8 and Arp 2 are extremely extended clusters with core radii which barely fit within the WFPC2 field of view. Nonetheless, our measured r_c for Arp 2 is in excellent agreement with all three previously published quantities. This, along with M54, demonstrates that even with γ severely under-estimated we can obtain useful measures of r_c , and leads us to have confidence in our core radii for the other Sagittarius clusters. Terzan 8 is interesting because the two previous measurements of r_c are respectively “little better than a guess” (Trager et al. 1995), and a by-eye estimate (Webbink 1985). Given the success of our fit to Arp 2, we feel that our new core radius measurement for Terzan 8, significantly larger than the two previous measurements, is the most reliable available value. Finally, for the Sagittarius clusters it is worthwhile noting that if we assume our calculated core radii to be accurate measurements, then given that γ is under-estimated for each of these clusters, it follows from Eq. 3 that a must also be an under-estimate of that value which would be measured for a fully extended profile. Therefore, like for the γ values, our measurements of a must also be considered lower limits.

4.1.2 Is Fornax 5 a post core-collapse cluster?

In Paper I, we identified several of the old LMC globular clusters as post core-collapse (PCC) candidates. A PCC cluster is characterized by an apparent power-law profile in its innermost region,

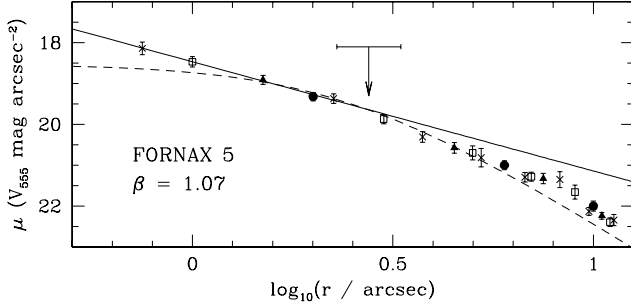


Figure 4. Power-law fit to the inner core of Fornax 5. The four different point styles represent the four annulus sets, as in Fig. 1. The best-fit EFF and power-law profiles are shown as is the power-law slope (β) and break radius (arrow) with error indicated. Because of the magnitude scale, the slope of the power-law model as plotted is 2.5β .

rather than a profile with a constant density core (such as a King or EFF profile). Many also show a distinct break at the transition to the power-law region. Studies of Galactic PCC clusters (see e.g., Lugger, Cohn & Grindlay (1995); Djorgovski & King (1986)) have shown typical power-law slopes in the range $0.6 < \beta < 1.0$, assuming the profiles go as $r^{-\beta}$. Similarly, in Paper I, our two best candidates (NGC 2005 and NGC 2019) had $\beta \approx 0.75$. We also measured typical break radii of ~ 1.3 pc.

As is evident in Fig. 1 and Fig. 2, the only clusters in the present sample which are compact enough to be PCC candidates are Fornax 3, 4, and 5, and M54. Our profile for M54 is incomplete in its inner region, so we cannot observe if it follows a power-law. Nevertheless, we observe no evidence of any break (1.3 pc $\sim 10''$), and no previous high-resolution profiles (such as that from Trager et al. (1995)) show any evidence for PCC structure. The Fornax clusters are more interesting, because this is the first study with sufficient resolution to identify any PCC structure – for the previous ground-based observations, atmospheric blur would have wiped out the innermost profile details on a scale of $\sim 2''$ or more. Fig. 1 shows that Fornax 3 and Fornax 4 are well fit by EFF profiles in their central regions, and neither shows evidence for a break at the expected radius. Fornax 5 however, does not appear well fit by an EFF model, with the measured profile showing a tell-tale deviation at its innermost two points.

A magnified plot of the core of the profile of Fornax 5 is presented in Fig. 4, together with an attempted power-law fit, and the best fitting EFF model. At less than $3''$ the power-law is clearly the more suitable model. The best-fitting slope is $\beta = 1.07$, slightly steeper than the range measured for Galactic PCC clusters. We estimate a break radius of $\log r_{\text{break}} = 0.44 \pm 0.08$, which translates to $r_{\text{break}} = 1.83 \pm 0.34$ pc – slightly larger than the typical break radius we measured for the LMC PCC candidates. Nonetheless, based on the evidence of Fig. 4, we believe that Fornax 5 is a solid PCC candidate, worthy of further attention. Interestingly, in Paper I, we estimated that 20 ± 7 per cent of the old LMC cluster population was in a PCC state, and similarly, Djorgovski & King (1986) estimated a PCC fraction of ~ 20 per cent for the Galactic globular clusters. Based on these numbers, it might be expected that ~ 1 cluster in either (or both) of the Fornax and Sagittarius systems be a PCC cluster – seemingly exactly what we have observed.

4.2 Luminosity and mass estimates

It is possible to estimate luminosities and masses for each cluster using the structural parameters obtained from the surface brightness profiles. The procedure for doing this, and the derivation of the equations involved, is detailed in Paper I. Briefly, we determined that for a cluster with an EFF surface brightness profile, the asymptotic luminosity is given by:

$$L_{\infty} = \frac{2\pi\mu_0 a^2}{\gamma - 2} \quad (4)$$

provided $\gamma > 2$. When $\gamma \approx 2$, the extrapolation $r \rightarrow \infty$ likely severely overestimates L_{∞} . It is therefore useful to derive a lower-limit for the total luminosity of a cluster. We decided that the enclosed luminosity within a cylinder of radius r_m along the line of sight, where r_m is the maximum radial extent measured for a given profile (see Table 5), was a suitable quantity, because this is essentially the directly observed luminosity of a given cluster. In Paper I, we showed that:

$$L_m = \frac{2\pi\mu_0}{\gamma - 2} \left(a^2 - a^{\gamma} (a^2 + r_m^2)^{-\frac{(\gamma-2)}{2}} \right) \quad (5)$$

To calculate L_{∞} and L_m , the central surface brightness μ_0 must be converted to physical units ($L_{\odot} \text{ pc}^{-2}$). Again in Paper I, we derived an expression for this:

$$\log \mu_0 = 0.4(V_{555}^{\odot} - \mu_{555}(0) + DM + A_V) + \log(SF^2) L_{\odot} \text{ pc}^{-2} \quad (6)$$

where DM is the distance modulus of the cluster concerned (Table 4, column 2), SF is its scale factor (arcsec pc^{-1} ; Table 4, column 5), A_V is the line of sight V -band extinction, and $V_{555}^{\odot} = +4.85$ is the F555W magnitude of the sun (see Paper I). To calculate A_V for each cluster, we use the colour excesses from Table 4 (either column 6 or 7), and the extinction laws described in Section 2.2.4.

The values for μ_0 , j_0 , L_{∞} , and L_m so calculated appear in Table 7. We note that these are F555W luminosities and luminosity densities. As discussed in Section 4.1, all of the Sagittarius clusters have $\gamma < 2$, because only their very central regions were imaged. This means that L_{∞} cannot be directly calculated for these clusters, because the integration which gives Eq. 4 is divergent. However, because the values of L_m are not strictly comparable between clusters or cluster sets (because r_m/r_c is different for each cluster), we would like to have some estimates of L_{∞} . We can obtain these by using a simple scaling approximation between clusters with similarly shaped profiles. First, we define a new quantity, L_c , which is simply Eq. 5 with r_m replaced by r_c . This represents the integrated luminosity of a cluster's core. Dividing this by Eq. 4 gives:

$$\frac{L_c}{L_{\infty}} = 1 - a^{(\gamma-2)} (a^2 + r_c^2)^{-\frac{(\gamma-2)}{2}} \quad (7)$$

For cluster Fornax 1, which has a core radius comparable to Terzan 8 and Arp 2, this fraction is ~ 0.4 . For the old clusters with the two largest core radii from Papers I and II (NGC 1841 and NGC 339) we calculate ~ 0.32 and ~ 0.35 respectively. Assuming Terzan 8 and Arp 2 have profiles which fall off similarly to the profiles of these three very extended clusters (i.e., γ in the range 5 – 8) we can adopt $L_c/L_{\infty} \sim 0.35$ and estimate L_{∞} by calculating L_c . These values are shown in Table 7. Terzan 7 is a more unusual cluster, with a small core radius but relatively low central density. Its profile seems most similar to the intermediate age clusters NGC 2193, NGC 2213, and Hodge 14, in the LMC. These three clusters typically have $L_c/L_{\infty} \sim 0.12$. Finally, M54 seems most similar to the compact old bar clusters from the LMC study. These clusters

Table 7. Luminosity and mass estimates calculated using the structural parameters from the best fitting EFF profiles.

Cluster	$\log \mu_0^a$ ($L_\odot \text{ pc}^{-2}$) ^b	Adopted [Fe/H]	Adopted M/L_V	$\log j_0$ ($L_\odot \text{ pc}^{-3}$) ^b	$\log L_\infty$ (L_\odot) ^{b,c}	$\log L_m$ (L_\odot) ^b	$\log \rho_0$ ($M_\odot \text{ pc}^{-3}$)	$\log M_\infty$ (M_\odot) ^c	$\log M_m$ (M_\odot)
Fornax 1	1.32 ± 0.02	-2.25	3.16	0.00 ± 0.07	4.07 ± 0.13	4.07 ± 0.13	0.50 ± 0.07	4.57 ± 0.13	4.57 ± 0.13
Fornax 2	2.39 ± 0.03	-1.65	3.20	1.31 ± 0.07	4.76 ± 0.12	4.75 ± 0.12	1.81 ± 0.07	5.26 ± 0.12	5.26 ± 0.12
Fornax 3	3.50 ± 0.03	-2.25	3.16	2.99 ± 0.06	5.06 ± 0.12	5.00 ± 0.11	3.49 ± 0.06	5.56 ± 0.12	5.50 ± 0.11
Fornax 4	3.20 ± 0.05	-1.65	2.69	$2.64^{+0.13}_{-0.12}$	4.69 ± 0.24	$4.67^{+0.23}_{-0.24}$	$3.07^{+0.13}_{-0.12}$	5.12 ± 0.24	$5.10^{+0.23}_{-0.24}$
Fornax 5	3.24 ± 0.06	-2.25	3.16	2.79 ± 0.11	4.76 ± 0.20	$4.67^{+0.17}_{-0.18}$	3.29 ± 0.11	5.25 ± 0.20	$5.17^{+0.17}_{-0.18}$
M54	4.23 ± 0.02	-1.65	3.22	3.97 ± 0.05	(5.70)	5.36 ± 0.08	4.48 ± 0.05	(6.21)	5.86 ± 0.08
Terzan 7	2.00 ± 0.02	-0.64	2.54	1.49 ± 0.07	(3.68)	$3.50^{+0.10}_{-0.11}$	1.90 ± 0.07	(4.08)	$3.91^{+0.10}_{-0.11}$
Terzan 8	1.37 ± 0.02	-2.25	3.14	$0.24^{+0.23}_{-0.21}$	(4.08)	$3.67^{+0.10}_{-0.14}$	$0.74^{+0.23}_{-0.21}$	(4.57)	$4.17^{+0.10}_{-0.14}$
Arp 2	1.16 ± 0.02	-1.65	2.85	$-0.13^{+0.25}_{-0.24}$	(4.18)	$3.59^{+0.09}_{-0.14}$	$0.33^{+0.25}_{-0.24}$	(4.64)	$4.04^{+0.09}_{-0.14}$

^a Corrected for reddening using the values from Table 4.^b Parameters with units of L_\odot are F555W luminosities (or luminosity densities).^c Values in parenthesis (the Sagittarius clusters) are calculated via a scaling estimate, as described in the text.

have an average $L_c/L_\infty \sim 0.15$. However, using this to estimate L_∞ for M54 yields a value smaller than our calculated L_m . This suggests that the asymptotic γ for M54 is shallower than those ($\gamma \sim 2.6$) for the LMC bar clusters, which makes sense seeing as there is probably a much stronger tidal field at the centre of the LMC than at the centre of the Sagittarius dwarf. We therefore calculate an upper limit for the mass of M54 by extrapolating its profile to the literature tidal radius from Table 6 and integrating via Eq. 5.

The L_∞ measurements agree well with previous such measurements in the literature. For example, Webbink (1985) lists the five Fornax clusters as having absolute integrated V magnitudes of $M_V = -5.23, -7.30, -8.19, -7.23$, and -7.38 , respectively. These correspond to integrated luminosities of $\log L_{tot} = 4.02, 4.85, 5.20, 4.82$, and 4.88 , respectively, which compare well with the L_∞ values derived in the present study. If anything, there is the tendency for a slight systematic under-estimate in our L_∞ values. This is possibly due to Webbink's slightly larger adopted distance (145 kpc), although we note that our technique of determining brightness profiles through star counts does certainly cause some luminosity to be missed. Specifically, the bright and faint limits of each observation exclude some stars from the profiles, leading to an under-estimate in μ_0 and hence L_∞ . For the Fornax clusters, the missing number of bright stars is negligible due to the inclusion of short exposures in the construction of the “master” frames. For the Sagittarius clusters no stars above approximately horizontal branch level were counted. At the faint end, typical limiting magnitudes for the Fornax clusters were $V_{555} \sim 26.5$ (i.e., $L \sim 0.5L_\odot$), and for the Sagittarius clusters were $V_{555} \sim 24$ (i.e., $L \sim 0.2L_\odot$). We expect the systematic errors from the missed contribution to L_∞ from saturated and unseen stars to be within the random (and other systematic) uncertainties discussed below.

For the Sagittarius clusters, Harris (1996) lists absolute integrated V magnitudes of $M_V = -10.01, -5.05, -5.05$, and -5.28 (for M54, Terzan 7, Terzan 8, and Arp 2 respectively), which correspond to integrated luminosities of $\log L_{tot} = 5.93, 3.95, 3.95$, and 4.18 . Again, the agreement with our derived values of L_∞ is close, especially given our estimation technique for these clusters.

By multiplying the appropriate luminosity values by a suitable mass-to-light ratio (M/L_V) for the cluster in question, estimates for the masses M_∞ and M_m , and the central density ρ_0 may be obtained. As previously (see Papers I and II), we determined

the M/L_V values from the evolutionary synthesis code of Fioc & Rocca-Volmerange (1997) (PEGASE v2.0, 1999), which determines the integrated properties of a synthetic stellar population as a function of age. We selected a single burst population, formed with constant metallicity and according to the IMF of Kroupa, Tout & Gilmore (1993) over the mass range 0.1 to $120M_\odot$. As in Papers I and II, we matched each cluster to the most suitable of the four available abundances in the evolutionary synthesis code – either $[\text{Fe}/\text{H}] \approx -2.25, -1.65, -0.64$, or -0.33 , based on the literature metallicities in Table 3 – and using the literature age estimates (also in Table 3) determined M/L_V . As demonstrated in Paper I, these calculations are relatively insensitive to the chosen metallicity, so we are confident in using the estimates in Table 3 even for clusters (such as Terzan 7) where there is some discrepancy between photometrically and spectroscopically determined metallicities. The M/L_V ratios are however, reasonably sensitive to the adopted age (as can be seen in the difference between the ratios for Fornax 2 and Fornax 4 – where Fornax 4 is assumed to be ~ 3 Gyr younger than Fornax 2), so uncertainties in the ages potentially translate into significant systematic errors in the assumed M/L_V ratios.

The total mass and central density values are also shown in Table 7. We estimated M_∞ for the Sagittarius clusters using the L_∞ values calculated as above. As in Papers I and II, the indicated errors in Table 7 reflect only the random uncertainties in (μ_0, γ, a) and do not include systematics such as those caused by uncertainties in ages or in distance moduli and reddenings. The largest of these latter errors – the ~ 10 per cent distance error for the Fornax clusters – results in at maximum a ~ 2 per cent error in μ_0 and a ~ 20 per cent error in L_∞ – both within the random uncertainties for these values.

5 THE DISTRIBUTION OF CORE RADII

In Papers I and II, we presented evidence for a trend in core radius with age for the cluster systems of both the LMC and SMC – namely that the spread in r_c increases dramatically with increasing age. In the context of identifying the cause of this trend, it is important to observe whether it exists uniquely in the Magellanic Clouds (which are themselves fairly atypical members of the Local

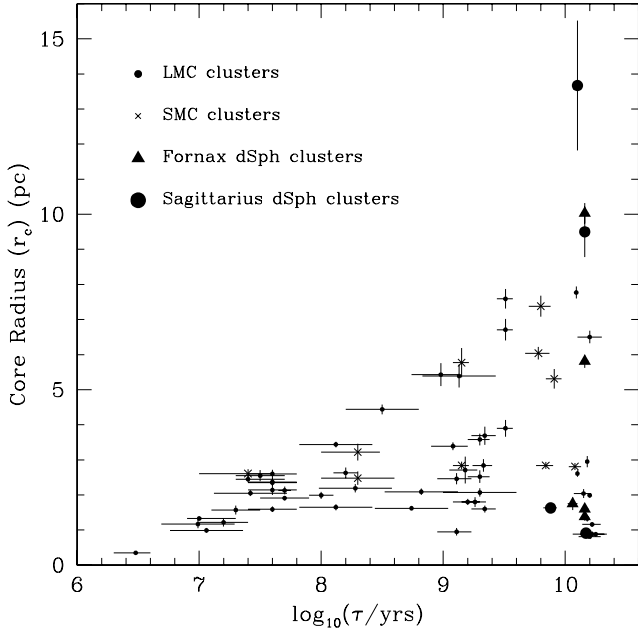


Figure 5. Core radius vs. age for the 53 LMC and 10 SMC clusters from Papers I and II (small filled circles and small crosses respectively) together with the Fornax and Sagittarius dSph globular clusters from the present paper (large filled triangles and large filled circles respectively). Points with no visible error-bars have uncertainties smaller than their symbol size. Apart from Arp 2, the spread in core radii for the oldest clusters is in good agreement between each sample. Arp 2 matches the LMC cluster Reticulum (not plotted), which has $r_c \sim 14.6$ pc (see text).

Group) or whether it extends to cluster systems in other galaxies. It is therefore very useful to take the results we have presented here for the Fornax and Sagittarius dSph globulars and compare them with those for the oldest clusters in the Magellanic systems.

An immediate qualitative comparison is possible by simply adding the Fornax and Sagittarius clusters to the radius-age plots from Papers I and II (Fig. 5). It is clear that the new clusters agree closely with the distribution observed for the Magellanic clusters, apart from Arp 2. Even this cluster is not unique however – it is well matched by the LMC cluster Reticulum (see below), which was not measured in the sample of Paper I.

It is worth noting briefly the result of de Grijs et al. (2002) who have demonstrated that the radius-age distribution persists even if only stars in the mass range $0.8 - 1.0 M_\odot$ are used to construct the radial profiles. This means that the reduced spread in core radius for the youngest clusters cannot be a result of their profiles being dominated by a few high luminosity mass-segregated stars. Similarly, de Grijs et al. show that the degree of mass segregation for LMC clusters *even of different ages* is very similar. In terms of our profile construction technique, this means that the omission of very faint (and in some cases very bright) stars from the star counts should not alter the derived structural parameters significantly (apart from a zero-point shift), and hence does not affect any analysis in terms of the radius-age trend. We are also justified in directly comparing the profiles of clusters of all ages.

A more detailed examination than that from the simple radius-age plot can be obtained by constructing cumulative distributions in r_c for the Sagittarius clusters, the Fornax clusters, and the old Magellanic Cloud clusters. When matching these distributions against

each other, it is important that we have cluster samples which are as complete as possible, otherwise selection effects may bias the results. We are confident that our sample of Fornax clusters is complete, and if we add Pal 12 to our group of Sagittarius clusters, this sample is also complete to the limits of present knowledge (although it is certainly possible that other outer halo globular clusters will be identified as former Sagittarius members in the future). Unfortunately, Pal 12 is, like Terzan 7, Terzan 8, and Arp 2, a very sparse cluster with a distinctly patchy appearance. Its structure therefore appears difficult to quantify, and there is a wide variation in literature measurements of r_c . Webbink (1985) lists $r_c \sim 28''$, while Chernoff & Djorgovski (1989) measure $r_c \sim 31''$. In contrast, Trager et al. (1995) have $r_c \sim 1''.7$, determined from a very ragged profile. Harris (1996) lists $r_c \sim 12''$ which is presumably some average of all available literature measurements. In the absence of other information, we will adopt this value – at Harris’s listed distance of 19.1 kpc it converts to $r_c \sim 1.1$ pc. Clearly, better measurements of this object are required, especially given its recently elevated status as a Sagittarius dSph cluster.

We also need to ensure that our samples of old Magellanic clusters are complete. In comparison with the youngest clusters in the Fornax and Sagittarius dSph systems (Terzan 7, ~ 7.5 Gyr; Pal 12, $\sim 7 - 8$ Gyr (Buonanno et al. 1998a; Rosenberg et al. 1999; Salaris & Weiss 2002)), we define “old” to include all clusters with $\tau \geq 7$ Gyr. This means that in addition to the twelve old LMC clusters from Paper I, we must definitely add the Reticulum cluster, which is coeval with the metal poor Galactic globulars (e.g., Walker (1992)) and has $r_c = 60 \pm 20''$ (Webbink 1985), corresponding to $r_c = 14.6 \pm 4.5$ pc at a distance modulus of 18.5. We must also add ESO 121-SC03, the only cluster to lie in the LMC age gap, with $\tau = 9 \pm 2$ Gyr and $r_c = 34 \pm 5''$ (Mateo, Hodge & Schommer 1986), which is $r_c = 8.3 \pm 1.2$ pc at the LMC distance. It is also necessary to mention NGC 1928 and NGC 1939, which are compact clusters in the LMC bar. The spectroscopic study of Dutra (1999) has shown that these two are likely to be old; however no CMDs or surface brightness profiles appear in the literature for either. For the moment therefore, we will not include them in our calculations – as we will see below, their presence or otherwise is not significant.

Unfortunately, the SMC cluster system is not as easy to quantify as the LMC system, partly because there is no age gap for the SMC clusters. In addition, as discussed in Paper II, the SMC clusters have not been extensively studied, and literature measurements of cluster ages and structural parameters are few and far between. The sample of Paper II included the only bona fide old SMC cluster (NGC 121), as well as four clusters with ages of $6 - 8$ Gyr (NGC 339, NGC 361, NGC 416, Kron 3). In addition, Mighell, Sarajedini & French (1998) have shown that the cluster Lindsay 1 has $\tau \sim 9$ Gyr, and that Lindsay 113 has $\tau \sim 5 - 6$ Gyr, while Piatti et al. (2001) show that Lindsay 38 has $\tau \sim 6$ Gyr. None of these clusters have high resolution brightness profiles in the literature; nor is it clear how many other massive SMC clusters might have $\tau \sim 7$ Gyr or greater. We are therefore unable to include the SMC clusters in the quantitative discussion below – once again the need for extra measurements of the clusters in this system is evident.

The cumulative distributions in r_c for the LMC old clusters and the Fornax and Sagittarius dSph clusters are shown in Fig. 6. Even without considering the uncertainties in the literature measurements of r_c discussed above, it is clear that the distributions match well, especially given the small sample sizes for the dSph clusters. There are several aspects worth considering in greater detail. Firstly, it should be noted that for the most compact Fornax

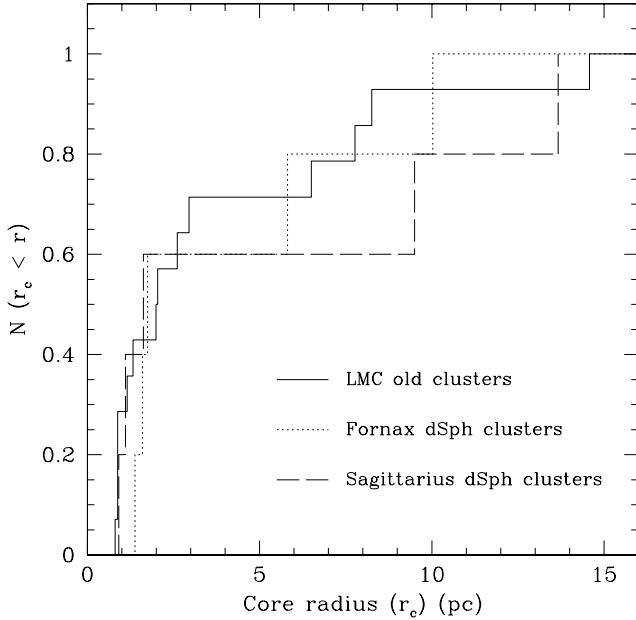


Figure 6. Cumulative distributions in r_c for old LMC clusters, and clusters in the Fornax and Sagittarius dwarf galaxies. Measurements for the Fornax clusters are taken from the present study, as are those for the Sagittarius clusters (except Pal 12 which is from the literature). Measurements for twelve of the fourteen LMC clusters are from Paper I; the remaining two are taken from the literature, as discussed in the text.

clusters, our core radius measurements are upper limits because of the resolution of our profiles. This means that the agreement in the distributions at small r_c is probably even better than shown. Similarly, we note that the measurements of r_c for the most compact LMC clusters from Paper I are also upper limits. Secondly, in Paper I we discussed the possibility that the radius-age distribution showed a bifurcation at ~ 100 Myr, so that the old clusters follow an almost bimodal distribution – that is, they can either be compact ($r_c \leq 3$ pc) or extended ($r_c \geq 7$ pc). We can see this distribution in the cumulative profile for the LMC clusters, as a flat region between ~ 3 and ~ 7 pc. It is possible that this is simply a small sample effect. However, it seems that both of the dSph cluster systems follow a similar distribution, with a dearth of clusters in the range $2 \leq r_c \leq 6$ pc. We also note that our measurements from Paper II show that the oldest SMC clusters also appear to have a grouped distribution, although again, it is likely that this sample is incomplete.

In terms of a direct comparison between the LMC and dSph cluster distributions, we can use the apparent grouping of clusters for a quantitative estimate. From Fig. 6 it is clear that ~ 65 – 70 per cent of old LMC clusters have $r_c < 3$ pc. This leads us to expect that in each dSph system, at most 0.7×5 clusters, or ~ 3 will have $r_c < 3$, which is exactly what we observe. A K-S test can provide a more rigorous assessment of how well the distributions match, although we note that such a test is not necessarily well suited to samples as small as those we are dealing with here. Nonetheless, applying a K-S test to the LMC and Fornax samples shows that they were drawn from the same distribution at ~ 97.5 per cent significance. If we ignore differences between the distributions for $r_c < 1.6$ pc (because of our resolution limits) this increases to > 99 per cent. Comparing the LMC and Sagittarius samples yields

a match at ~ 75 per cent significance, with the largest difference occurring between the two distributions near $r_c = 9$ pc – a region where stochastic effects (and measurement errors) are large. Finally, comparing the Fornax and Sagittarius samples shows that they are similar at ~ 70 per cent significance. If we again neglect the differences for $r_c < 1.6$ pc, the significance increases to ~ 99 per cent. We note that adding one or two clusters to the small r_c end of the LMC distribution (e.g., NGC 1928 and/or NGC 1939) would decrease the significances of the match between the LMC and dSph samples slightly, but the agreement would remain good. Similarly, increasing the core radius of Pal 12 to $\sim 30''$, or ~ 3 pc (as discussed above), again would not influence the agreement between the distributions significantly. The greatest differences in Fig. 6 always occur for large r_c , especially given the resolution limits, and this region is effectively unchanged by the addition, removal, or shifting of a couple of clusters at the low end of the plot.

We conclude therefore that the distribution of old clusters we observed for the LMC in Paper I, and to a certain extent for the SMC in Paper II, is not unique to the Magellanic systems but rather appears universal, at least in the satellite galaxies of the Milky Way. Not only do all the cluster systems we have observed possess expanded clusters, they possess them in the same proportion, irrespective of the mass of the host galaxy, and its isolation (or otherwise). While this does not show that the radius-age trend of the Magellanic clusters is universal, it does demonstrate that the end-point of this trend matches the end-points of whatever paths cluster evolution has followed in the Sagittarius and Fornax dwarf galaxies. Given the differences between the environments local to these two galaxies (Fornax is relatively isolated, while Sagittarius is engaged in strong tidal interactions with the Milky Way) and that of the more massive LMC, it is clear that external influences are unlikely to be the driving force behind the radius-age trend, in agreement with the simulations of Wilkinson et al. (2003). If changing formation conditions are the key to the puzzle, as suggested by these authors, the implication from the present work is that these conditions were the same across the entire local region at the epoch of initial cluster formation. Given that the first burst of cluster formation does appear to have occurred simultaneously across both dwarf spheroidals, the Milky Way, and the LMC, this is not an outlandish suggestion. New N -body cluster evolution calculations are of course required to further explore the radius-age trend and its end-points, as well as the possible effects of varying formation conditions. Such simulations are presently in progress. Similarly, it is important to investigate the SMC system in more detail observationally, as described above. Finally, by far the largest sample of local globular clusters belongs to the Milky Way. An analysis of the structures of these clusters in the context of what we have observed for the external systems is currently underway.

6 SUMMARY AND CONCLUSIONS

We have presented surface brightness profiles for all the globular clusters in the Fornax and Sagittarius dwarf galaxies, derived from archival *HST* WFPC2 observations. The profiles were constructed similarly to those for the LMC and SMC clusters we studied in Papers I and II, with only minor modifications to the procedure to account for special properties of the present data. From the surface brightness profiles, we have determined structural parameters for each cluster, including their core radii and estimates for their total luminosities and masses. These data, along with the surface brightness profiles are available on-line

at http://www.ast.cam.ac.uk/STELLARPOPS/dSph_clusters/. Our measurements of core radii are generally in reasonable agreement with previous lower resolution measurements in the literature. However, we have found the core radius of Terzan 7 to be smaller than previously determined, and that for Terzan 8 to be somewhat larger. We have also presented evidence that Fornax cluster 5 is a post core-collapse candidate.

Examining the two cluster systems in the context of the radius-age trend which we highlighted in Papers I and II, we find that the distribution of cluster core radii in both dwarf galaxies matches that for the old LMC clusters within the limits set by measurement errors and the small sample sizes. While this is not evidence for the dSph clusters having evolved via the same radius-age trend we observed for Magellanic Cloud clusters, it does indicate that the end-points of the structural evolution of clusters in these four systems are equivalent. The fact that this equivalence exists even though the four parent galaxies have very different masses and formation histories, and have been influenced by the Milky Way to varying degrees, suggests that it is not strong external influences which have primarily determined these evolutionary end-points. By inference, the radius-age trend in the Magellanic clusters is therefore unlikely to be driven by external forces.

ACKNOWLEDGMENTS

ADM would like to acknowledge the support of a Trinity College ERS grant and a British government ORS award. This paper is based on observations made with the NASA/ESA *Hubble Space Telescope*, obtained from the data archive at the Space Telescope Institute. STScI is operated by the association of Universities for Research in Astronomy, Inc. under the NASA contract NAS 5-26555.

REFERENCES

- Arp H. C., 1965, in Blaauw A., Schmidt M., eds, *Galactic Structure*. University of Chicago Press, Chicago, p. 401
- Beauchamp D., Hardy E., Suntzeff N. B., Zinn R., 1995, *AJ*, 109, 1628
- Buonanno R., Corsi C. E., Fusi Pecci F., Hardy E., Zinn R., 1985, *A&A*, 152, 65
- Buonanno R., Corsi C. E., Pulone L., Fusi Pecci F., Richer H. B., Fahlman G. G., 1995a, *AJ*, 109, 663
- Buonanno R., Corsi C. E., Fusi Pecci F., Richer H. B., Fahlman G. G., 1995b, *AJ*, 109, 650
- Buonanno R., Corsi C. E., Pulone L., Fusi Pecci F., Bellazzini M., 1998, *A&A*, 333, 505
- Buonanno R., Corsi C. E., Zinn R., Fusi Pecci F., Hardy E., Suntzeff N. B., 1998, *ApJ*, 501, L33
- Buonanno R., Corsi C. E., Castellani M., Marconi G., Fusi Pecci F., Zinn R., 1999, *AJ*, 118, 1671
- Cardelli J. A., Clayton G. C., Mathis J. S., 1989, *ApJ*, 345, 245
- Chernoff D. F., Djorgovski S., 1989, *ApJ*, 339, 904
- Da Costa G. S., Armandroff T. E., 1995, *AJ*, 109, 2533
- de Grijs R., Gilmore G. F., Mackey A. D., Wilkinson M. I., Beaulieu S. F., Johnson R. A., Santiago B. X., 2002, *MNRAS*, in press
- Demers S., Kunkel W. E., Grondin L., 1990, *PASP*, 102, 632
- Demers S., Irwin M. J., Kunkel W. E., 1994, *AJ*, 108, 1648
- Dinescu D. I., Majewski S. R., Girard T. M., Cudworth K. M., 2000, *AJ*, 120, 1892
- Djorgovski S., King I. R., 1986, *ApJ*, 305, L61
- Dolphin A. E., 2000a, *PASP*, 112, 1383
- Dolphin A. E., 2000b, *PASP*, 112, 1397
- Dubath P., Meylan G., Mayor M., 1992, *ApJ*, 400, 510
- Dutra C. M., Bica E., Clariá J. J., Piatti A. E., 1999, *MNRAS*, 305, 373
- Elson R. A. W., 1991, *ApJS*, 76, 185
- Elson R. A. W., 1992, *MNRAS*, 256, 515
- Elson R. A. W., Fall S. M., Freeman K. C., 1987, *ApJ*, 323, 54
- Elson R. A. W., Freeman, K. C., Lauer, T. R., 1989, *ApJ*, 347, L69
- Fioc M., Rocca-Volmerange B., 1997, *A&A*, 326, 950
- Forbes D. A., Masters K. L., Minniti D., Barmby P., 2000, *A&A*, 358, 471
- Harris W. E., 1996, *AJ*, 112, 1487
- Hodge P. W., 1961, *AJ*, 66, 83
- Ibata R. A., Gilmore G., Irwin M. J., 1994, *Nature*, 370, 194
- Ibata R. A., Wyse R. F., Gilmore G., Irwin M. J., Suntzeff N. B., 1997, *AJ*, 113, 634
- Irwin M., Hatzidimitriou D., 1995, *MNRAS*, 277, 1354
- Jørgensen U. G., Jimenez R., 1997, *A&A*, 317, 54
- King I., 1962, 67, 471
- Kroupa P., Tout C. A., Gilmore G. F., 1993, *MNRAS*, 262, 545
- Layden A. C., Sarajedini A., 2000, *AJ*, 119, 1760
- Lugger P. M., Cohn H. N., Grindlay J. E., 1995, *ApJ*, 439, 191
- Mackey A. D., Gilmore G. F., 2002a, *MNRAS*, in press (Paper I)
- Mackey A. D., Gilmore G. F., 2002b, *MNRAS*, in press (Paper II)
- Martínez-Delgado D., Zinn R., Carrera R., Gallart C., 2002, *ApJ*, 573, L19
- Mateo M., Hodge P., Schommer R. A., 1986, *ApJ*, 311, 113
- Mighell K. J., Sarajedini A., French R. S., 1998, *AJ*, 116, 2395
- Montegriffo P., Bellazzini M., Ferraro F. R., Martins D., Sarajedini A., Fusi Pecci F., 1998, *MNRAS*, 294, 315
- Ortolani S., Gratton R., 1990, *A&AS*, 82, 71
- Piatti A. E., Santos Jr. J. F. C., Clariá J. J., Bica E., Sarajedini A., Geisler D., 2001, *MNRAS*, 327, 792
- Press W. H., Teukolsky S. A., Vetterling W. T., Flannery B. P., 1992, *Numerical Recipes in C: The Art of Scientific Computing*, (2nd Edition). Cambridge University Press, New York
- Rodgers A. W., Roberts W. H., 1994, *AJ*, 107, 1737
- Rosenberg A., Saviane I., Piotto G., Aparicio A., 1999, *AJ*, 118, 2306
- Salaris M., Weiss A., 2002, *A&A*, 388, 492
- Sarajedini A., Layden A. C., 1995, *AJ*, 109, 1086
- Sarajedini A., Layden A. C., 1997, *AJ*, 113, 264
- Smith E. O., Neill J. D., Mighell K. J., Rich R. M., 1996, *AJ*, 111, 1596
- Terzan A., 1968, *C.R. Acad. Sci. Ser. B*, 267, 1245
- Trager S. C., Djorgovski S., King I. R., 1993, in Djorgovski S. G., Meylan G., eds, *ASP Conf. Ser. Vol. 50, Structure and Dynamics of Globular Clusters*. Astron. Soc. Pac., San Francisco, p. 347
- Trager S. C., King I. R., Djorgovski S., 1995, *AJ*, 109, 218
- Walker A. R., 1992, *AJ*, 103, 1166
- Webbink R. F., 1985, in Goodman J., Hut P., eds, *Proc. IAU Symp. 113, Dynamics of Star Clusters*. Kluwer, Dordrecht, p. 541
- Wilkinson M. I., Hurley J. R., Mackey A. D., Gilmore G. F., Tout C., 2003, in preparation
- Zinn R., in Smith G. H., Brodie J. P., eds, *ASP Conf. Ser. Vol. 48, The Globular Cluster-Galaxy Connection*. Astron. Soc. Pac., San Francisco, p. 303
- Zinn R. J., West M. J., 1984, *ApJS*, 55, 45

This paper has been produced using the Royal Astronomical Society/Blackwell Science \LaTeX style file.